Sensors & Transducers, Vol. 213, Issue 6, June 2017, pp. 38-45

Sensors & Transducers

Published by IFSA Publishing, S. L., 2017
http://www.sensorsportal.com

Study of Propylene Glycol, Dimethylformamide and Formaldehyde Vapors Sensors Based on MWCNTs/SnO_2 Nanocomposites

[1] Zaven Adamyan, [1] Artak Sayunts, [1] Vladimir Aroutiounian,
[1] Emma Khachaturyan, [1] Arsen Adamyan, [2] Martin Vrnata,
[2] Přemysl Fitl and [2] Jan Vlček
[1] Yerevan State University, Department of Physics of Semiconductors and Microelectronics,
Center of Semiconductor Devices and Nanotechnologies, 1 A. Manoukian, 0025 Yerevan, Armenia
[2] University of Chemistry and Technology, Department of Physics and Measurement Technology,
Technická 5, 166 28 Prague 6, Czech Republic
[1] Tel.: +37460710311, fax: +37460710355
[1] E-mail: kisahar@ysu.am

Received: 22 May 2017 /Accepted: 22 June 2017 /Published: 30 June 2017

Abstract: We present results of our research works related to the study of thick-film multiwall carbon nanotube/tin oxide nanocomposite sensors of propylene glycol (PG), dimethylformamide (DMF) and formaldehyde (FA) vapors derived using hydrothermal synthesis and sol-gel methods. Investigations of response/recovery characteristics in the 50-300 °C operating temperature range reveal that the optimal operating temperature for PG, DMF and FA vapor sensors, taking into account both high response and acceptable response and recovery times, are about 200 and 220 °C, respectively. A sensor response dependence on gas concentration in all cases is linear. The minimal propylene glycol and dimethylformamide gas concentrations at which the perceptible signal was registered by us were 13 ppm and 5 ppm, respectively.

Keywords: MWCNTs/SnO_2, Gas, Vapor, Sensor, Dimethylformamide, Propylene glycol, Formaldehyde.

1. Introduction

There are various harmful and hazardous matter vapors, which have a major role in diverse spheres such as environmental protection, industrial manufacture, medicine, as well as national defense. As an illustration, propylene glycol (PG) is an excellent solvent for many organic compounds and is used as an active ingredient in engine coolants and antifreeze, brakes, paints, enamels and varnishes, and in many products as a solvent or surfactant. It can also be found in cosmetics, perfumes, as well as in pharmaceuticals.

Another example is the dimethylformamide (DMF) which is used as a solvent in vinyl resins, adhesives, pesticide and epoxy formulations; which purifies and separates of acetylene, 1,3-butadiene, acid gases and aliphatic hydrocarbons, also in the production of polyacrylic or cellulose triacetate fibres and pharmaceuticals or in the production of polyurethane resin for synthetic leather [1].

Formaldehyde (FA) is a colorless, water-soluble gas with a pungent odor which used in making building materials and many household products such as particleboard, plywood and fiberboard, glues and adhesives, textiles, paper and their product coatings.

Besides, formaldehyde can serve an intermediate in the manufacture of industrial chemicals. It can also be found as a preservative in some foods and in products, such as antiseptics, medicines, and cosmetics [2].

DMF, PG and FA have a huge impact on human organs (e.g. liver, skin, eyes and kidneys [1-4]). PG can cause nausea and vomiting, headache, dizziness and fainting. Moreover, it is known as a combustible liquid, which can explode in fire. FA gas can cause burning sensations of the eyes, nose, and throat, coughing, wheezing, nausea, skin irritation. Besides, exposure to relatively high amounts of formaldehyde can increase the risk of leukemia and even cause to some types of cancer in humans.

Due to the information noted above, PG, DMF and FA gas sensors have a huge application for detecting and continuous monitoring of these gases, in the spheres where they are used.

As a result of our carefully conducted analysis of the literature data, we did not find any works related to research and development of resistive sensors of PG and DMF gases. There are only sensors working in other principle (for example sensors working on modification of color of the substance), which is incompatible for contemporary technic, while, resistive gas sensors made from metal oxides have advantages such as electric signal, measurement of concentration, small sizes, low power consumption, high sensitivity, and long reliability [5-7].

As opposed to this case, there are many various types of FA gas sensors. For instance, FA gas sensors based on graphene or polymers which are working at room temperature [8-9]. On the other hand, FA gas sensors based on metal-oxide materials have advantages mentioned above. However pure metal-oxide structures react on FA at higher operating temperatures (300-400 ^{o}C) [10-11] or at room temperature with the assistance of UV LED [12-13].

Nanomaterials, as carbon nanotubes (CNTs), metal-oxide nanoparticles, nanotubes, nanowires and other various nanopatterns formation [14-19] are widely used in gas sensing for their excellent responsive characteristics, mature preparation technology, and low cost of mass production. Due to the covering of CNTs walls with metal-oxide nanoparticles, specific surface area of such gas-sensitive nanocomposites increases more. Moreover, nanochannels in the form of hollows of CNTs promote penetration of gas molecules deeper down in the nanocomposite sensitive layer [20]. Hence, it can be expected that application in gas sensors technology of nanocomposite structures composed of metal oxide functionalized with CNTs should enhance the gas sensor parameters, such as gas response, response, recovery times, and operating temperatures.

Our recent works related to the study of gas sensors based on multiwall carbon nanotubes/tin oxide (MWCNTs/SnO_2) nanostructures are also argued in [17, 21-22]. The choice of tin oxide as a component of SnO_2/MWCNTs nanocomposite structure is conditioned by the fact that SnO_2 is well known and studied basic material for metal-oxide gas sensors (see, for example [5, 16, 23-24]). We expected that coating of functionalized MWCNTs with SnO_2 nanoparticles with admissible, (close to double Debay length) sizes [23-27] should provide the improved performance of the gas sensor and lowered the temperature of its operating.

Here, we present the characteristics of the PG, DMF and FA vapor sensors based on ruthenated thick-films MWCNT/SnO_2 nanocomposite structures. The choice of corresponding processing technique, treating conditions and regimes for CNTs functionalization, as well as modification of thick films surface with Ru catalyst, are described below in the second section. Results of the measurements of PG, DMF and FA vapor sensors and their discussions are given in the third section.

2. Experimental Development

MWCNTs/SnO_2 nanocomposite material processing and thick-film sensor manufacturing technology on the base of this nanocomposite are presented in this section. It is shortly described both the MWCNTs preparation and its covering with SnO_2 nanoparticles obtained by using the hydrothermal method. Ruthenium catalyst deposition technology is also shown here.

MWCNTs membranes which were used for the preparation of nanocrystalline MWCNTs/SnO_2 powder were kindly provided to us by our colleagues from the University of Szeged, Hungary. MWCNTs were prepared by the decomposition of acetylene (CVD method) using Fe, Co/$CaCO_3$ catalyst [28-29]. This growth procedure using $CaCO_3$ catalyst enables a highly efficient selective formation of clean MWCNTs, suitable for effective bonding between CNT and metal-oxide, particularly, for SnO_2 precursors.

For a functionalization of nanotube walls with oxygen-containing hydroxyl (OH), carbonyl (C=O), and carboxylic (COOH) functional groups, MWCNTs from the membranes were transferred to slurry in HNO_3/H_2SO_4 acids mixture during 1 h. Such a functionalization of the CNTs is very important and necessary for the following synthesis of SnO_2 nanoparticles on the MWCNTs walls since these oxygen-containing groups act as sites for the nucleation of nanoparticles. After rinsing with distilled water and drying at 80^{o}C, MWCNTs were poured and treated in deionized water in the ultrasonic bath for 5 min.

The preparation of nanocomposite materials with a hydrothermal method was carried out in two steps. Firstly, purified MWCNTs were dispersed in water via sonication. Then, a calculated amount of precursor of the $SnCl_2 \cdot 2H_2$ was dissolved in another beaker in water, whereupon 3 cm^3 HCl was added to the solution. The choice of water as a solvent, instead of e.g. ethanol, was preferably for us in the view of expected improvement in gas sensing characteristics, taking into account the fact that cover the overwhelming parts of CNTs with SnO_2 nanoparticles is ensured at that [30]. In the next step, the MWCNT's suspension and the solution of the precursor were mixed and sonicated for 30 min. For preparing the nanocomposites, we poured the above-mentioned solutions into autoclaves, where hydrothermal synthesis was carried out at 150 °C for 1 day. At the end of this procedure, all obtained nanocomposite powders were filtered and dried at 90 °C for 5 h. The final mass ratios of the nanocomposite MWCNTs/SnO_2 obtained with the hydrothermal method in this study were 1:200, respectively. The hydrothermal synthesis process is presented in details in [17, 31-32].

The paste for the thick film deposition made by mixing powders with α-terpineol ("Sigma Aldrich") and methanol was printed on the chemically treated surface of the alumina substrate over the ready-made Pt interdigitated electrodes. The thin-film Pt heater was formed on the back side of the substrate. Then, the obtained composite structures were cut into 3×3 mm pieces. After that, the drying and annealing processes of the resulting thick films were carried out in two stages: The first step is the heating of thick films up to 220 °C with the 2 $^{\circ}C\times min^{-1}$ rate of temperature rise and holding for 3h and then increasing in temperature until 400 °C with the $1^{\circ}C\times min^{-1}$ rate and holding for 3 h. In the second step, the thick-film specimens were cooled down in common with the oven.

After annealing and cooling processes, the surface of MWCNTs/SnO_2 thick films was ruthenated by dipping samples into the 0.01 M $RuOHCl_3$ aqueous solution for 20 min whereupon drying at 80 °C for 30 min. Then, the annealing treatment was carried out again by the same method noticed above. The choice of the ruthenium as a catalyst was determined by its some advantages [17, 22, 31]. At the final stage, ruthenated MWCNT/SnO_2 chips were arranged in TO-5 packages and the gas sensors would be ready to measurements after bonding of leads.

3. Results and Discussions

Some results of the nanocomposite sensors have been presented during the international conference in Nice [33]. In this paper we introduce the extended version of our investigations. Surface morphology studies, as well as gas sensor characteristics, are shown in this section, but the performances of PG, DMF and FA sensors are separately considered. Also, the dependence of electrical resistance of the sensors on operating temperature, as well as values of responses, response and recovery times of the sensors at various operating temperatures or target gas concentrations are shown here too.

3.1. Material Characterization

The morphologies of the prepared SnO_2/MWCNT nanocomposite powders with diverse compounds were studied by scanning electron microscopy using Hitachi S-4700 Type II FE-SEM equipped with a cold field emission gun operating in the range of 5–15 kV. The presence of an oxide layer was confirmed by SEM-EDX. Furthermore, the crystalline structure of the inorganic layer was also studied by an X-ray diffraction method using the Rigaku Miniflex II diffractometer (angle range: 2θ [°]=10–80 utilizing characteristic X-ray (CuKα) radiation). Results of these investigations were presented in [17, 31] more detailed. Here, we are only noting that average crystalline size of SnO_2 nanoparticles estimated from SEM images and XRD patterns are less than 12 nm but the average diameter of non-covered by SnO_2 nanoparticles CNTs was about 40 nm.

3.2. Gas Sensing Characteristics

Gas sensing properties of the MWCNTs/SnO_2 nanocomposite structures were measured by home-made developed and computer-controlled static gas sensor test system [27]. The sensors were reheated and studied at different operating temperatures. When the electrical resistance of all studied sensors was stable, the vital assigned amount of compound in the liquid state for sensors testing was injected by a microsyringe in measurement chamber. Moreover, the target matters were introduced into the chamber on the special hot plate designed for the quick conversion of the liquid substance to its gas phase. After its resistance reached a new constant value, the test chamber was opened to recover the sensors in air. The sensing characteristics were studied in the 20-300 °C operating temperature range and the gas response of the sensors determines as R_a/R_g, where R_a and R_g are the electrical resistances in the air and in target gas-air atmosphere, respectively. The response and recovery times are determined as the time required for reaching the 90 % resistance changes from the corresponding steady-state value of each signal.

3.3. PG Vapor Sensor Characteristics

Firstly, we should determine the operating temperature of the sensors. As a result of measurements of the sensor resistance in air and air/gas environment, the maximal response to 650 ppm PG vapor was revealed at 200 °C operating temperature (Fig. 1 and Fig. 2).

Good repeatability of the sensor response can be seen from Fig. 3, where the electrical resistance change of PG sensor vs time measured upon cyclic exposure of 650 ppm PG vapors in air at 200 °C operating temperature is presented.

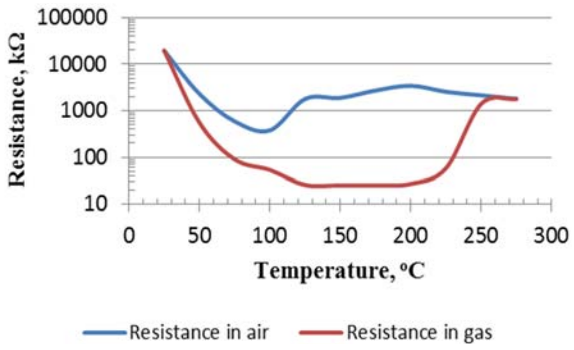

Fig. 1. Dependence of electrical resistance change of MWCNTs/SnO$_2$ thick-film sensors on operating temperature.

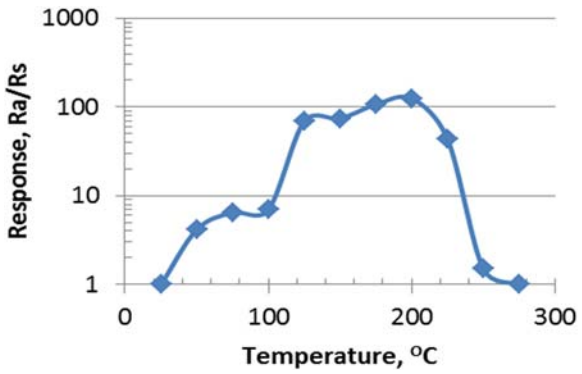

Fig. 2. Response of MWCNTs/SnO$_2$ thick-film PG sensors vs operating temperature.

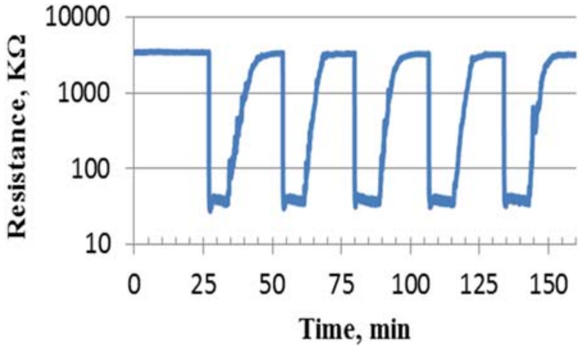

Fig. 3. The electrical resistance change of MWCNTs/SnO$_2$ thick-film PG sensors vs time measured upon cyclic exposure of 650 ppm PG vapors in air at 200°C operating temperature.

Changes of the response and recovery times depending on operating temperature are presented in Fig. 4 and Fig. 5.

Dependence of the resistance and response of MWCNTs/SnO$_2$ sensor on PG vapor concentration is shown in Fig. 6 and Fig. 7, respectively. As it is obvious from the figures, the sensor response occurs down to small target gas concentrations (13 ppm) but the response approximately linearly depends on the gas concentration.

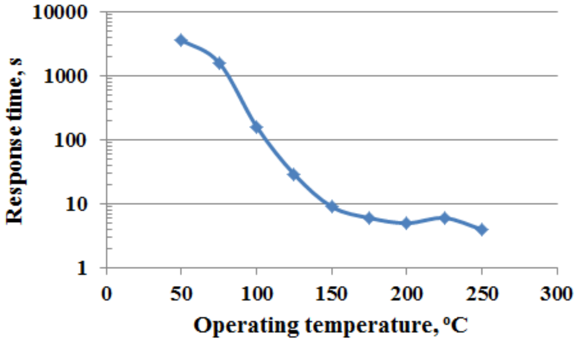

Fig. 4. Response time vs operating temperature.

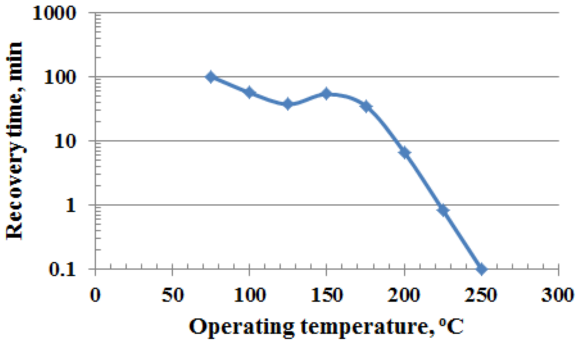

Fig. 5. Recovery time vs operating temperature.

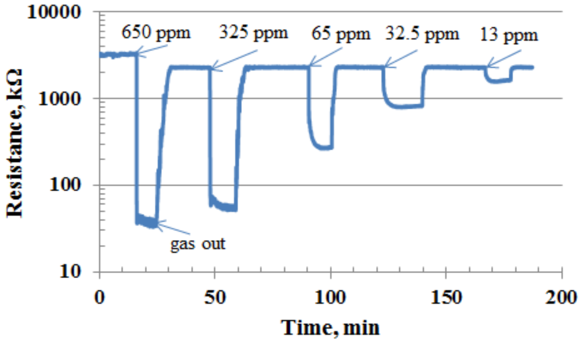

Fig. 6. The response/recovery curves observed at different PG concentrations exposure measured at 200°C operating temperature.

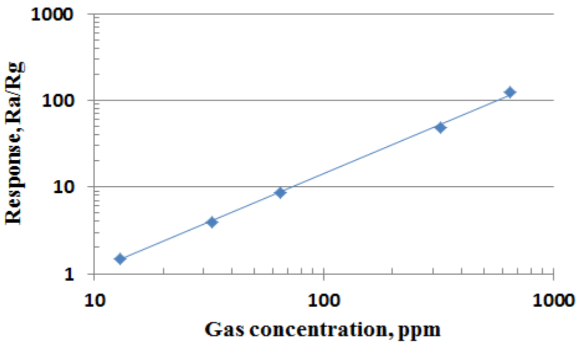

Fig. 7. Dependence of the response of MWCNTs/SnO$_2$ PG vapor sensor on gas concentration measured at 200°C operating temperature.

3.4. DMF Vapor Sensor Characteristics

The sensor response derived as a result of 500 ppm DMF vapor exposure versus operating temperature is presented in Fig. 8.

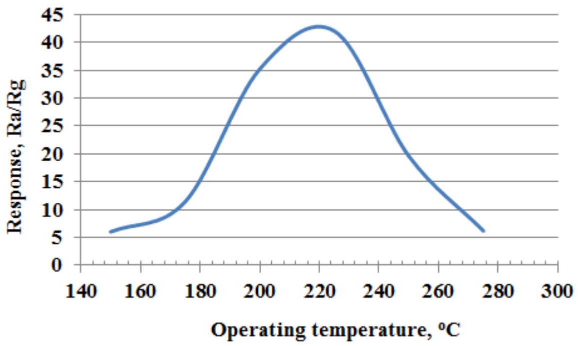

Fig. 8. Response vs operating temperature at 500 ppm DMF vapor exposure.

It can be seen that maximal response, in this case, is registered in the range of 210-225 °C. Dependence of the sensor response on versus DMF vapor concentration is also linear (Fig. 9).

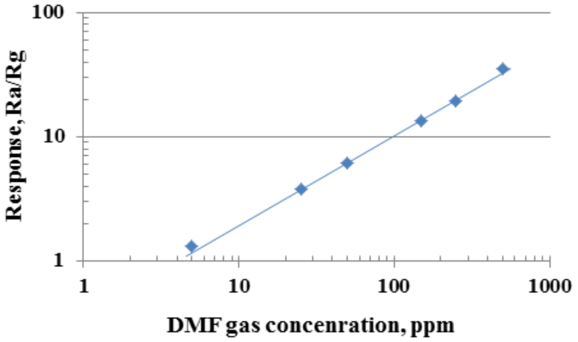

Fig. 9. Dependence of the response of MWCNTs/SnO_2 DMF vapor sensor on gas concentration measured at 200 °C operating temperature.

3.5. FA Vapor Sensor Characteristics

As a result of measurements of the sensor resistance in air and air/gas environment, the maximal response to FA vapor was revealed in the range of 200-225 °C operating temperatures (Fig. 10). Dependence of the response and recovery times of MWCNTs/SnO_2 FA vapor sensor on operating temperature is shown in Fig. 11.

Dependences of the resistance and response of MWCNTs/SnO_2 sensor on FA vapor concentration are shown in Fig. 12 and Fig. 13, respectively. As it is obvious from the figures, the sensor response increases with increasing concentration of the influencing FA gas, and this response rise occurs linearly.

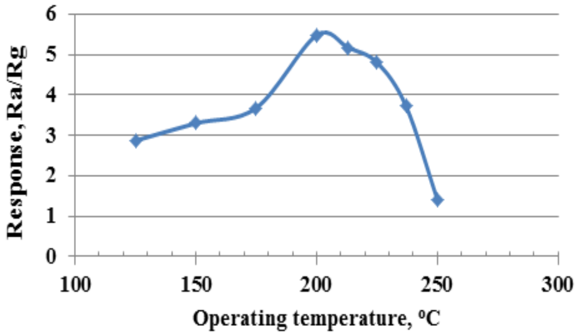

Fig. 10. Response of MWCNTs/SnO_2 thick-film FA sensors vs operating temperature.

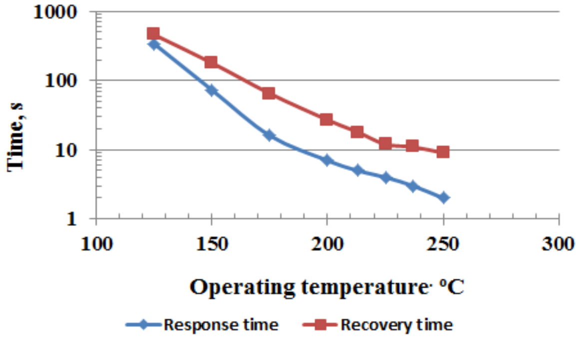

Fig. 11. Dependence of the response and recovery times of MWCNTs/SnO_2 FA vapor sensor on operating temperature.

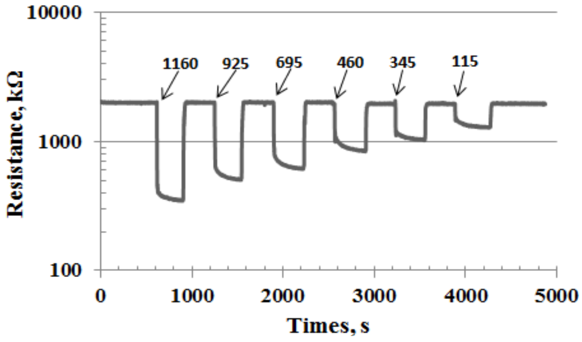

Fig. 12. The response/recovery curves observed at different FA gas concentrations exposure measured at 200 °C operating temperature.

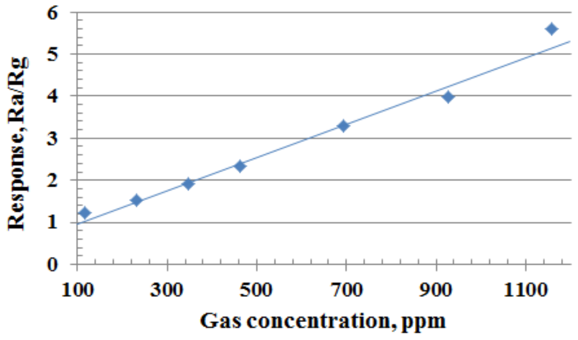

Fig. 13. Dependence of the response of MWCNTs/SnO_2 FA vapor sensor on gas concentration measured at 200 °C operating temperature.

3.6. Comparison

Comparison of responses of MWCNTs/SnO_2 sensors to 650 ppm PG, 500 ppm DMF and 1160 ppm FA vapors exposure vs operating temperature is shown in Fig. 14.

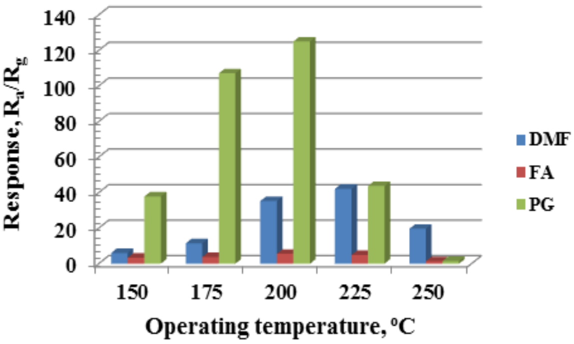

Fig. 14. Comparison of responses of MWCNTs/SnO_2 sensors to 650 ppm PG, 500 ppm DMF and 1160 ppm FA vapors exposure at various operating temperatures.

As it is shown from the Fig. 14, Sensors demonstrate the best response against PG and FA vapors at 200 °C operating temperature and against DMF vapor at 225 °C operating temperature.

3.7. On Possible Mechanism of Gas Sensitivity

It is known that the attachment of carboxyl groups on the surface of MWCNTs is effective in nucleation and trapping the other materials including tin oxide nanoparticles. As it was shown earlier, COOH groups attached on the surface of MWCNTs have a strong interaction with alcohol vapors resulting hydrogen bond between COOH groups and the OH groups of alcohol molecules [17-22]. This hydrogen bond should be removed by increasing the temperature, which contributes to long recovery times in MWCNTs/SnO_2 sensors.

The increase in response with an increase in the operating temperature of the sensor is observed until the maximum value is reached. With the subsequent increase in operating temperature, desorption of chemisorbed oxygen ions takes place and gas response decreases; the recovery time decreases, too.

MWCNTs nanochannels play a smaller role at relatively more content of SnO_2 in the nanocomposite (as in our case), as nanotubes are closed by plenty of SnO_2 nanoparticles. Due to it, accessibility of gas molecules penetration to MWCNTs nanochannels through the metal-oxide thick film is very difficult. Therefore, the gas response is mainly determined by a number of metal-oxide nanoparticles and a considerable amount of surface adsorption sites. MWCNTs only prevent the formation of agglomerates of SnO_2 and ensure the development of the surface because of repulsive forces between the carboxyl groups adsorbed on it.

The oxidation reaction of PG and DMF vapors on the nanocomposite surface could be represented as follows, respectively:

$$C_3H_8O_2(g) + 8O^- \rightarrow 3CO_2(g) + 4H_2O(g) + 8e^-$$

and

$$4C_3H_7NO(g) + 42O^- \rightarrow 12CO_2(g) + 4NO_2(g) + 14H_2O(g) + 42e^-$$

At the temperature corresponding to the highest response, the reactivity of the target gas molecules is proportional to the speed of diffusion into the sensing layer. Hence, the target gas has the chance to sufficiently penetrate into the sensing layer and react with an appropriate speed. The competition between the amount of adsorbed target gases and their oxidation rate supports the maximum response and its sharp decline. With the following increase in operating temperature, desorption of the adsorbed oxygen ions from the surface of the sensor is increased. It follows that less amount of oxygen ions presents on the surface of SnO_2, might take part in reaction with target gases at higher operating temperature. Therefore, the response falls at high operating temperatures. Furthermore, it influences the physical properties of the semiconducting sensor material. For instance, at higher temperatures the carrier concentration increases (resulting from the release of electrons back to the conduction band in consequence of desorption of adsorbed oxygen) and the Debye length decreases. This may also be one of the possible reasons for the rise in Rg curve in Fig. 1, which leads to the decrease in response at higher temperatures. Although molecular weights of both considered target gases are close to each other, the quantity of carbon atoms is the same. Nevertheless, the response from DMF vapors influences less due to many adsorbed oxygen ions, resulted from the chemical decomposition, which demands for the full oxidation reaction. Thus, the 1:200 weight ratios of the nanocomposite sensor components with relatively large amount of SnO_2 particles promote an initiation of a sufficiently large quantity of ionized adsorption centers, which ensure relatively high response to DMF gas exposure.

FA gas sensing mechanism is not fully researched so far. It is proposed that the HCHO sensing process can be described by the commonly accepted gas sensing mechanism for n-type semiconducting metal oxides including SnO_2. Namely, as a result of adsorption-oxidation and desorption processes sensor surface is covered by chemisorbed oxygen ions, such as O^- and O^{2-}. When sensor exposed with FA gas HCHO molecules interact with the adsorbed oxygen according to the following reactions.

$$HCHO + 2O^- \rightarrow H_2O + CO_2 + 2e^-$$

$$HCHO + 2O^{2-} \rightarrow H_2O + CO_2 + 4e^-$$

These reactions lead to enhance the free electron concentration which causes the decrease of the resistance of SnO_2.

As for selectivity, this nanocomposite sensor demonstrates cross-sensitivity to some alcohols, such as butanol, methanol and ethanol at 200 °C operating temperature [21, 31]. Unlike existing other type PG, DMF and FA sensors, presented nanocomposite sensor is able to measure the concentration of mentioned gases in the atmosphere.

4. Conclusions

In this paper, we have carried out the investigation of obtaining ruthenated MWCNTs/SnO_2 thick-film nanocomposite sensors using hydrothermal synthesis and sol-gel technologies. It is revealed that studied sensors give a sufficiently high response to such harmful and hazardous gases as PG, DMF and FA at relatively low operating temperatures. The fast response of the sensors (at the order of seconds) and acceptable recovery times are observed under all gas concentrations influence at 200 °C operating temperature. The minimal PG, DMF and FA gas concentrations at which the perceptible signal is registered are 13 ppm, 5 ppm and 115 ppm, respectively.

Due to the linear dependence of the response on the concentration of PG, DMF and FA vapors, it is possible to easily measure the concentration of mentioned gases in the atmosphere.

Acknowledgements

This work was supported by NATO EAP SFPP 984.597.

References

[1]. A. Fiorito, F. Larese, S. Molinari, T. Zanin, Liver function alterations in synthetic leather workers exposed to dimethylformamide, *American Journal of Industrial Medicine*, Vol. 32, No. 3, 1997, pp. 255-260.

[2]. M. A. Lefebvre, W. J. Meulingb, R. Engel, M. C. Coroamac, G. Rennerc, W. Pape, G. J. Nohynek, Consumer inhalation exposure to formaldehyde from the use of personal care products/cosmetics, *Regulatory Toxicology and Pharmacology*, Vol. 63, Issue 1, 2012, pp. 171-176.

[3]. G. Malaguarnera, E. Cataudella, M. Giordano, G. Nunnari, G. Chisari, M. Malaguarnera, Toxic hepatitis in occupational exposure to solvents, *World Journal of Gastroenterology*, 2012, Vol. 18, Issue 22, pp. 2756-2766.

[4]. H. Y. Chang, T. S. Shih, Y. L. Guo, C. Y. Tsai, P. C. Hsu, Sperm function in workers exposed to N,N-dimethylformamide in the synthetic leather industry, *Fertil Steril*, Vol. 81, Issue 6, 2004, pp. 1589-1594.

[5]. V. M. Aroutiounian, in Advanced Sensors for Safety and Security, A. Vaseashta, S. Khudaverdyan (eds.), *NATO Science for Peace and Security, Series B: Physics and Biophysics*, Chapter 9, 2012.

[6]. G. F. Fine, L. M. Cavanagh, A. Afonja, R. Binions, Metal oxide semi-conductor gas sensors in environmental monitoring, *Sensors*, Vol. 10, Issue 6, 2010, pp. 5469-5502.

[7]. G. Korotcenkov, S. H. Han, B. K. Cho, Material design for metal oxide chemiresistive gas sensors, *Journal of Sensor Science and Technology*, Vol. 22, No. 1, 2013, pp. 1-17.

[8]. W. Y. Chuang, S. Y. Yang, W. J. Wu, C. T. Lin, A Room-Temperature Operation Formaldehyde Sensing Material Printed Using Blends of Reduced Graphene Oxide and Poly(methyl methacrylate), *Sensors*, Vol. 15, No. 11, 2015, pp. 28842-28853.

[9]. J. Flueckiger, F. K. Ko, K. C. Cheung, Microfabricated Formaldehyde Gas Sensors, *Sensors*, Vol. 9, No. 11, 2009, pp. 9196-9215.

[10]. K. Xu, D. Zeng, S. Tian, S. Zhang, C. Xie, Hierarchical porous SnO_2 micro-rods topologically transferred from tin oxalate for fast response sensors to trace formaldehyde, *Sensors and Actuators B: Chemical*, Vol. 190, 2014, pp. 585-592.

[11]. H. J. Park, N. J. Choi, H. Kang, M. Y. Jung, J. W. Park, K. H. Park, D. S. Lee, A ppb-level formaldehyde gas sensor based on CuO nanocubes prepared using a polyol process, *Sensors and Actuators B: Chemical*, Vol. 203, 2014, pp. 282–288.

[12]. F. C. Chung, R. J. Wu, F. C. Cheng, Fabrication of an Au@SnO_2 core–shell structure for gaseous formaldehyde sensing at room temperature, *Sensors and Actuators B: Chemical*, Vol. 190, 2014, pp. 1-7.

[13]. X. Li, X. Li, J. Wang, S. Lin, Highly sensitive and selective room-temperature formaldehyde sensors using hollow TiO_2 microspheres, *Sensors and Actuators B: Chemical*, Vol. 219, 2015, pp. 158-163.

[14]. V. M. Aroutiounian, Gas sensors based on functionalized carbon nanotubes, *Journal of Contemporary Physics (Armenian Academy of Sciences)*, Vol. 50, No. 4, 2015, pp. 333-354. *Izvestiya NAN Armenii, Fizika*, Vol. 50, No. 4, 2015, pp. 448-475.

[15]. M. M. Arafat, B. Dinan, S. A. Akbar, A. S. M. A. Haseeb, Gas sensors based on one dimensional nanostructured metal-oxides: A Review, *Sensors*, Vol. 12, No. 6, 2012, pp. 7207-7258.

[16]. G. Korotcenkov, S. D. Han, B. K. Cho, V. Brinzari, Grain size effects in sensor response of nanostructured SnO_2 and In_2O_3-based conductometric thin film gas sensor, *Critical Reviews in Solid State and Materials Sciences*, Vol. 34, Issue 1-2, 2009, pp. 1-17.

[17]. V. M. Aroutiounian, A. Z. Adamyan, E. A. Khachaturyan, Z. N. Adamyan, K. Hernadi, Z. Pallai, Z. Nemeth, L. Forro, A. Magrez, E. Horvath, Study of the surface-ruthenated SnO_2/MWCNTs nanocomposite thick-film gas sensors, *Sensors and Actuators B: Chemical*, Vol. 177, 2013, pp. 308-315.

[18]. S. A. Feyzabad, A. A. Khodadadia, M. V. Naseh, Y. Mortazavi, Highly sensitive and selective sensors to volatile organic compounds using MWCNTs/SnO_2, *Sensors and Actuators B: Chemical*, Vol. 166–167, 2012, pp. 150-155.

[19]. N. V. Hieu, L. T. B. Thuy, N. D. Chien, Highly sensitive thin film NH_3 gas sensor operating at room temperature based on SnO_2/MWCNTs composite, *Sensors and Actuators B: Chemical*, Vol. 129, 2008, pp. 888-895.

[20]. X. Bai, H. Ji, P. Gao, Y. Zhang, X. Sun, Morphology, phase structure and acetone sensitive properties of

copper-doped tungsten oxide sensors, *Sensors and` Actuators B: Chemical*, Vol. 193, 2014, pp. 100-106.

[21]. V. M. Aroutiounian, Z. N. Adamyan, A. G. Sayunts, E. A. Khachaturyan, A. Z. Adamyan, Study of MWCNT/SnO_2 nanocomposite acetone and toluene vapor sensors, in *Proceedings of the 17th International Conference on Sensors and Measurement Technology (SENSOR'15)*, Nierenberg, Germany, 19-21 May 2015, pp. 836-841.

[22]. Z. N. Adamyan, A. G. Sayunts, E. A. Khachaturyan, V. M. Aroutiounian, Study of nanocomposite thick-film butanol vapor sensors, *Journal of Contemporary Physics (Armenian Academy of Sciences),* Vol. 51, Issue 2, 2016, pp. 143-149.

[23]. V. M. Aroutiounian, Metal oxide hydrogen, oxygen and carbon monoxide sensors for hydrogen setups and cells, *International Journal of Hydrogen Energy,* Vol. 32, Issue 9, 2007, pp. 1145-1158.

[24]. P. Shankar, J. Bosco, B. Rayappan, Gas sensing mechanism of metal oxides: The role of ambient atmosphere, type of semiconductor and gases - A review, *Science Letters*, Vol. 4/126, 2015, pp. 1-18.

[25]. C. Xu, J. Tamaki, N. Miura, N. Yamazoe, Grain size effects on gas sensitivity of porous SnO_2-based elements, *Sensors and Actuators B: Chemical*, Vol. 3, No. 2, 1991, pp. 147-155.

[26]. A. Z. Adamyan, Z. N. Adamyan, V. M. Aroutiounian, Preparation of SnO_2 films with thermally stable nanoparticles, *Sensors*, Vol. 3, 2003, pp. 438-442.

[27]. A. Z. Adamyan, Z. N. Adamyan, V. M. Aroutiounian, A. H. Arakelyan, J. Turner, K. Touryan, Sol–gel derived thin-film semiconductor hydrogen gas sensor, *International Journal of Hydrogen Energy*, Vol. 32, No. 16, 2007, pp. 4101-4108.

[28]. E. Couteau, K. Hernadi, J. W. Seo, L. Thien-Nga, Cs. Mikó, R. Gáal, L. Forró, CVD synthesis of high-purity multiwalled carbon nanotubes using $CaCO_3$ catalyst support for large-scale production, *Chemical Physics Letters*, Vol. 378, No. 1-2, 2003, pp. 9-17.

[29]. A. Magrez, J. W. Seo, R. Smajda, M. Mionić, L. Forró, Catalytic CVD Synthesis of Carbon Nanotubes: Towards High Yield and Low Temperature Growth, *Materials* Vol. 3, No. 11, 2010, pp. 4871-4891.

[30]. Z. Nemeth, B. Reti, Z. Pallai, P. Berki, J. Major, E. Horvath, A. Magrez, L. Forro, K. Hernadi, Chemical challenges during the synthesis of MWCNT-based inorganic nanocomposite materials, *Physica Status Solidi (B) Basic Research*, Vol. 251, Issue 12, 2014, pp. 2360-2365.

[31]. V. M. Aroutiounian, Z. N. Adamyan, A. G. Sayunts, E. A. Khachaturyan, A. Z. Adamyan, K. Hernadi, Z. Nemeth, P. Berki, Comparative study of VOC sensors based on ruthenated MWCNT/SnO_2 nanocomposites, *International Journal of Emerging Trends in Science and Technology (IJETST)*, Vol. 01, Issue 08, 2014, pp. 1309-1319.

[32]. Z. Nemeth, Z. Pallai, B. Reti, Z. Balogh, O. Berkesi, K. Baan, A. Erdohelyi, E. Horvath, G. Veréb, A. Dombi, L. Forró, K. Hernadi, Synthesis, Comparative Characterization and Photocatalytic Application of SnO_2/MWCNT Nanocomposite Materials, *Journal of Coating Science and Technology*, Vol. 1, No. 2, 2014, pp. 137-150.

[33]. Z. Adamyan, A. Sayunts, V. Aroutiounian, E. Khachaturyan, A. Adamyan, M. Vrnata, P. Fitl, J. Vlček, Study of Propylene Glycol and Dimethylformamide Vapors Sensors Based on MWCNTs/SnO_2 Nanocomposites, in *Proceedings of the Second International Conference on Advances in Sensors, Actuators, Metering and Sensing (ALLSENSORS 2017)*, Nice, France, 19-23 March 2017, pp. 44-49.

Published by International Frequency Sensor Association (IFSA) Publishing, S. L., 2017
(http://www.sensorsportal.com).